V European Conference on Computational Fluid Dynamics
ECCOMAS CFD 2010
J. C. F. Pereira and A. Sequeira (Eds)
Lisbon, Portugal, 14-17 June 2010

FLOW-CONTROLLED DETAILED CHEMISTRY TABULATION FOR THE LARGE EDDY SIMULATION OF NON-PREMIXED TURBULENT COMBUSTION

N. Enjalbert, P. Domingo and L. Vervisch

CORIA – CNRS & INSA de Rouen
Technopôle du Madrillet – BP 12, 76801 St Etienne du Rouvray, France
e-mail: enjalbert@coria.fr

Key words: Turbulent combustion, residence time, mixing, detailed chemistry tabulation, LES

Abstract. *This work is an attempt to take into account flow timescales, namely a residence time and a mixing time, in the description of turbulent combustion for Large-Eddy Simulations (LES). The history of the chemistry-turbulence interaction, parameterized by these timescales, is reproduced by means of a Partially-Stirred Reactor (PaSR) model and the resulting density-weighted averages of temperature, source terms and species mass fractions are tabulated. This approach is tested in the LES of a lifted methane-air jet flame in a vitiated co-flow.*

1 INTRODUCTION

A key challenge in modeling the dynamics of turbulent combustion for LES lays in how to account for the reactive flow history. The subgrid-scale (SGS) distributions, required for an evaluation of the resolved thermodynamic fields (temperature, species mass fractions, source terms), are the result of a history of turbulence-chemistry interaction. The different modeling approaches tackle this issue in different ways. On one side, the transported pdf methods[1] are designed precisely so as to follow the individual history of fluid elements, by tracking a modelled Lagrangian evolution of stochastic particles. A large number of particles is desirable for a good level of accuracy and, since the Lagrangian transport is computed on-the-fly, this method is a quite costly one. Towards the other side of the pdf modeling landscape, numerous methods offer smaller computational requirements by invoking relevant conditioning hypotheses. They reduce the number of degrees of freedom conferred on the turbulence-chemistry interaction, and in turn the simulation cost. Furthest on this way are some presumed pdf methods which rely on estimating the statistical properties of the distribution, such as averages and variances for the PCM formulation[2]. In this approach the history of the flow is handled through its effect on the statistical moments of the subgrid-scale distribution, which are assumed to be relevant conditioning variables. An easy look-up table procedure can then be used in the simulation, but assumptions on parameter correlations are necessary, and the number of degrees of freedom of the problem is therefore limited.

In this work, a new conditioning of the filtered fields is proposed, which directly accounts for properties of the flow history. Characteristic timescales are introduced: a residence time τ_{res} and a mixing time τ_{mix}, which quantify respectively the duration of the chemistry-turbulence interaction and the average intensity of the turbulence which the fluid particles have been submitted to along their trajectories. In this study, a flamelet hypothesis is invoked and the FPI formulation[3] adopted, which enables a description of chemistry with a mixture fraction Z and a progress variable Y_c. Simulations of a PaSR reproducing the characteristic evolution of the reactive flow particles are carried out and generate distributions and average chemical quantities, which, as an output, are stored in a four-dimensional $(\widetilde{Z}, \widetilde{Y}_c, \tau_{\text{res}}, \tau_{\text{mix}})$ look-up table to be accessed from the LES.

In a first section, the definition and properties of the residence and mixing timescales are presented. The formulation of the PaSR model is then given in a second section, along with the approach for the tabulation of its output. The properties of the output table are examined in a third section, and its insertion into an LES detailed in a fourth and last one.

2 RESIDENCE TIME AND MIXING TIME

2.1 Residence time

Let a scalar ϕ be defined by the Lagrangian equation

$$\frac{\mathrm{d}\phi}{\mathrm{d}t}(\underline{x},t) = S(\underline{x},t)\,. \tag{1}$$

It may be seen as the property of a single, identifiable particle, and measures the accumulation of the source field S on its trajectory $\mathcal{T} : t \mapsto \underline{x}(t)$; for an initial value ϕ_0, $\phi = \phi_0 + \int_{\mathcal{T}} S(\underline{x}(t),t)\mathrm{d}t$. Considering now ϕ as a Eulerian field, defined on any test volume of the flow as its ensemble average value on the enclosed particles, it verifies the following conservation equation:

$$\frac{\partial \rho\phi}{\partial t} + \underline{\nabla}\cdot(\rho\phi\underline{u}) = \underline{\nabla}\cdot(\rho D\underline{\nabla}\phi) + \rho S\,. \tag{2}$$

With this result, some important information on the history of the flow can be retrieved in a numerical simulation from simple transport and diffusion equations.

A direct, commonly used[4], application is the evaluation of the local average age of the flow particles since their entry in the flow, a scalar of the kind defined in Eq. 1:$\int_{\mathcal{T}}\mathrm{d}t$, obtained for $S = 1$. The residence time as defined in this study aims at measuring the duration of the chemistry-turbulence interaction, and therefore indexes the increase on the mixture fraction field: $S_Z^+ = 1 \times (1 - \delta(Z)\delta(Z-1))$. The residence time field verifies

$$\frac{\partial \rho\tau_{\mathrm{res}}}{\partial t} + \underline{\nabla}\cdot(\rho\tau_{\mathrm{res}}\underline{u}) = \underline{\nabla}\cdot(\rho D\underline{\nabla}\tau_{\mathrm{res}}) + \rho S_Z^+\,. \tag{3}$$

2.2 Trajectory-averaged mixing time

Also, the trajectory average of any quantity Q, defined for each particle as

$$\langle Q\rangle_{\mathcal{T}} = \frac{\int_{\mathcal{T}} Q(\underline{x}(t),t)\mathrm{d}t}{\int_{\mathcal{T}}\mathrm{d}t} \tag{4}$$

may be written $\langle Q\rangle_{\mathcal{T}} = Q^{\mathrm{I}}/\tau_{\mathrm{res}}$, where the integral Q^{I} is of the aforementioned kind and verifies Eq. 1 with $S = Q$. The Eulerian field of $\langle Q\rangle_{\mathcal{T}}$ may be computed by making, for the ensemble averaging, the approximation $\left\langle Q^{\mathrm{I}}/\tau_{\mathrm{res}}\right\rangle \simeq \left\langle Q^{\mathrm{I}}\right\rangle / \left\langle \tau_{\mathrm{res}}\right\rangle$, and solving $\left\langle Q^{\mathrm{I}}\right\rangle$ and τ_{res} from Eq. 2 and Eq. 3. This approach can be applied as an instrument to characterize the turbulence history of a fluid element in the flow. In the context of LES, where the large scales of velocity and scalar fields are resolved and the smaller scales modelled, a local mixing timescale τ^*_{mix} may be defined. It characterizes the intensity of the turbulence in the inertial and viscous ranges and its SGS variance reduction effect[5]

$$\tau^*_{\mathrm{mix}} = \frac{\Delta^2}{2(D+D_t)}\,, \tag{5}$$

where Δ is the LES filter size and $D_t \sim \Delta^2(\widetilde{s}_{ij}\widetilde{s}_{ij})^{1/2}$ the modeled turbulent diffusivity. Along a trajectory, the variance v of a characteristic passive scalar verifies instantaneously $\mathrm{d}v/\mathrm{d}t = -v/\tau^*_{\mathrm{mix}}$, and it is therefore $1/\tau^*_{\mathrm{mix}}$ whose role is linear. The average mixing level a fluid element has been submitted to in the flow histories of its particles may then be measured by $\tau_{\mathrm{mix}} = (\langle 1/\tau^*_{\mathrm{mix}}\rangle_{\mathcal{T}})^{-1} = \tau_{\mathrm{res}}/\left(1/\tau^*_{\mathrm{mix}}\right)^{\mathrm{I}}$, where $(1/\tau^*_{\mathrm{mix}})^{\mathrm{I}}$ verifies

$$\begin{aligned}\frac{\partial \rho(1/\tau^*_{\mathrm{mix}})^{\mathrm{I}}}{\partial t} + \underline{\nabla}\cdot\left(\rho(1/\tau^*_{\mathrm{mix}})^{\mathrm{I}}\underline{u}\right) = \\ \underline{\nabla}\cdot\left(\rho D\underline{\nabla}(1/\tau^*_{\mathrm{mix}})^{\mathrm{I}}\right) + \frac{\rho}{\tau^*_{\mathrm{mix}}}\,.\end{aligned} \tag{6}$$

2.3 Behavior in a jet

The simulations presented in this paper were all performed on a structured LES solver based on the framework of that of Domingo et al.[6,7] and Godel et al.[8]. The jet inlet diameter is $D = 4.57$ mm, with a bulk inlet velocity of 100 m.s^{-1} and a coflow of 5.5 m.s^{-1}. The mesh is composed of 1,950,000 cells.

The behavior of the introduced timescales in the Cabra et al.[9] configuration of a jet flame is shown in Fig. 1.

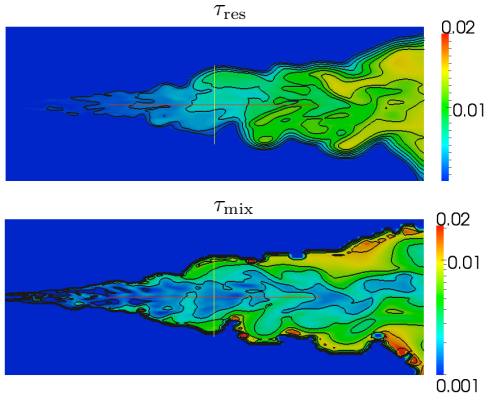

Figure 1: Instantaneous fields of τ_{res} and τ_{mix}.

3 REACTOR MODEL AND TABULATION METHOD

The Flow-Controlled Chemistry Tabulation (FCCT) approach stems from the idea that the aforementioned residence time τ_{res} and mixing timescale $\tau_{\mathrm{mix}} = (\langle 1/\tau^*_{\mathrm{mix}}\rangle_{\mathcal{T}})^{-1}$ are relevant conditioning variables for the turbulence-chemistry interaction. The SGS distributions lying behind thus conditioned filtered quantities are generated using Monte-Carlo computations of a PaSR. They aim at simulating a representative evolution of fluid elements from the inlet to a position where the mixing and residence timescales are known.

Joint distributions of the chemical parameters are generated, in one time, before the LES run, thanks to a tabulation method consistent with the conditioning hypothesis. The details of the procedure are presented below.

3.1 PaSR model definition

The system is composed of $N = 100$ "particles". Each particle is a sample point in the composition-temperature space, situated on the low-dimensional manifold describing the laminar flamelet structure. It is described by the two parameters Z and Y_c, which, within the flamelet framework, are sufficient to define all relevant quantities. If particle k's properties are marked by the superscript $^{(k)}$, the density $\rho^{(k)}$, temperature $T^{(k)}$, mass fraction of species i $Y_i^{(k)}$, are all functions of $(Z^{(k)}, Y_c^{(k)})$ and can be directly determined by interpolation from a flamelet table computed separately. Moreover, each particle has an age $a^{(k)}$ equal to the time it has spent in the reactor since its entry. The Favre-averaged value of a quantity Q in the system reads

$$\widetilde{Q} = \frac{\sum_{k=1}^{N} \rho^{(k)} Q^{(k)}}{\sum_{k=1}^{N} \rho^{(k)}} \,. \tag{7}$$

This discrete system is submitted to three processes: reaction, mixing and inflow/outflow. They are respectively controlled by a chemical timescale τ_{che} (inherent to the flamelet structure), an instantaneous mixing timescale $\tau_{\mathcal{M}}$ and an injection timescale $\tau_{\mathcal{R}}$. The equations verified by the k-th particle of the system, marked by the superscript $^{(k)}$, read:

$$\frac{\mathrm{d}Z^{(k)}}{\mathrm{d}t} = 0 + M_Z^{(k)} + R_Z^{(k)} \tag{8}$$

$$\frac{\mathrm{d}Y_c^{(k)}}{\mathrm{d}t} = \dot{\omega}_{Y_c}^{(k)} + M_{Y_c}^{(k)} + R_{Y_c}^{(k)} \tag{9}$$

where the rhs terms respectively model chemical reaction, mixing and inflow/outflow. The interaction between particles is carried by the mixing term, whereas chemistry and inflow/ouflow are applied to particles independently from their counterparts.

In an approach similar to that by Ren et al.[10], the system evolution is solved by a time marching scheme of time step Δt, with three fractional steps. Chemical reaction and mixing are solved as continuous processes on time intervals between two integer values of $t/\Delta t$, and a splitting scheme which ensures quadratic accuracy is used[11]. The inflow/outflow fractional step occurs at these discrete times. The implementation of these processes is described in detail below.

• The chemical reaction is modelled by a source term inserted in the Y_c equation (Eq. 9), which, as all others quantities, is obtained from the FPI laminar flamelet computation. It can more explicitly be written as

$$\dot{\omega}_{Y_c}^{(k)} = \dot{\omega}_{Y_c}^{\text{FPI}}(Z^{(k)}, Y_c^{(k)}) \,. \tag{10}$$

This source term carries the microscale flame structure, including the information of the intricate diffusion and reaction effects in laminar premixed combustion.

• The mixing in the PaSR is carried out by an EMST model[12]. Based on the construction of the Euclidian Minimum-Spanning Tree on a subset of particles, it is local in the (Z, Y_c) space, and is thus expected to realistically render the mixing, by intermediate-scale vortices, of spatially neighboring flames. If the set of particle k's neighbors in the EMST is denoted by $\mathcal{N}_k$, the mixing terms in Eqs. 8-9 are such that the system variance $V = Z_v + Y_{cv} = \widetilde{ZZ} - \widetilde{Z}\widetilde{Z} + \widetilde{Y_cY_c} - \widetilde{Y}_c\widetilde{Y}_c$, decreases at a characteristic rate $\tau_{\mathcal{M}}$:

$$\frac{\mathrm{d}V}{\mathrm{d}t} = -\frac{V}{\tau_{\mathcal{M}}} \,. \tag{11}$$

The instantaneous mixing time $\tau_{\mathcal{M}}$ obeys a distribution law $f_{\mathcal{M}}$ controlled by the average mixing timescale τ_{mix}, such that $\int_0^\infty f_{\mathcal{M}}(\tau)/\tau \mathrm{d}\tau = 1/\tau_{\mathrm{mix}}$. In this study the simple choice $\tau_{\mathcal{M}} = \tau_{\mathrm{mix}}$ is made.

• An inflow/outflow law is applied to the system, which controls the injection and removal of particles into and from the active contents of the reactor. It is a formulation of the boundary conditions of the dynamic system. At each time step, a replacement event takes place with probability $p_{\mathcal{R}}$: a number $N_{\mathcal{R}}$ of particles is picked and replaced by "fresh" ones, of age $a = 0$ and properties $Z_0, Y_{c,0}$. It is stated here that the probability to be picked is uniform among the particles, and heedless to their age or other criteria. This process is piloted by the instantaneous injection time $\tau_{\mathcal{R}} = \Delta t \times N/(p_{\mathcal{R}} N_{\mathcal{R}})$. The choice of $f_{\mathcal{R}}$, the law controlling $\tau_{\mathcal{R}}$, and of the inlet conditions, is of central importance for the dynamics of the reactor.

The purpose of this PaSR modeling is to reproduce, in the composition space, the temporal development of the chemical properties of the particles along their trajectories in the turbulent flow. The dynamics of the average properties of the reactor must therefore reproduce as closely as possible those observed in the actual flow. To that purpose, looking at how the resolved composition variables $\widetilde{Z}$ and $\widetilde{Y}_c$ depend in the flow on the residence time provides much insight on the dynamics of their temporal development. In Fig. 2, these quantities are presented as scatter plots versus the resolved τ_{res}, at a fixed time. The shape of these structures does not vary significantly with time. It appears clearly that all values of the filtered mixture fraction are bounded by a decreasing function of τ_{res}. At age zero, only pure fluid is encountered, $\widetilde{Z} = 0$ or 1; this corresponds to the fuel inlet and the $Z = 0$ boundary of the jet along its development, and stems from the fact that the source term is non-zero only if $\widetilde{Z}(1 - \widetilde{Z}) \neq 0$. Very quickly, the whole $[0; 1]$ range is filled, but as the residence time increases, at positions going deeper into the jet and farther downstream, the mixture fraction is bounded by a maximum value which goes decreasing. This is a clear illustration of turbulence homogenizing the mixture along trajectories in the flow, and the τ_{res} parameter distinctly evidences this behavior.

Aiming at reproducing this phenomenon, two choices are made for the PaSR simulation. In terms of inlet conditions, the reactor is set to start with only fuel particles, of age zero,

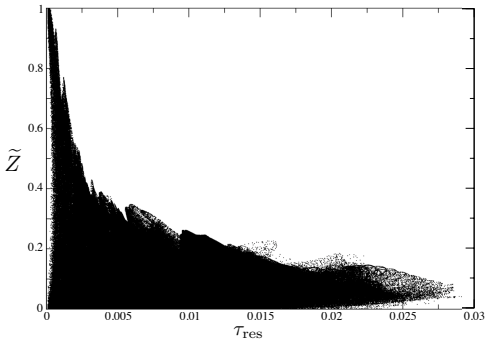

Figure 2: Scatter plot of the mixture fraction against the residence time τ_{res} from an arbitrary instantaneous snapshot of the LES results.

and fresh oxydizer is then randomly injected as the mixture grows older and mixes, so that the reactor's $\widetilde{Z}$ evolves from 1 to 0, and the age from 0 to a value determined by the rate of injection. When $\widetilde{Z}$ reaches 0, the reactor is reset to its initial configuration and the process starts again. As far as the injection dynamics are concerned, then, the law $f_{\mathcal{R}}$ is made a function of the average mixture fraction: it is tuned in such a way that the instantaneous injection time $\tau_{\mathcal{R}}$ varies between $\tau_{\mathcal{R},\mathrm{min}} = 10^{-4}$ s and a $\tau_{\mathcal{R},\mathrm{max}}(\widetilde{Z})$, and that the output scatter plot is close to that from the LES. In the present case $\tau_{\mathcal{R},\mathrm{max}}$ varies between 3×10^{-3} for high Z values and 0.05 s for low Z.

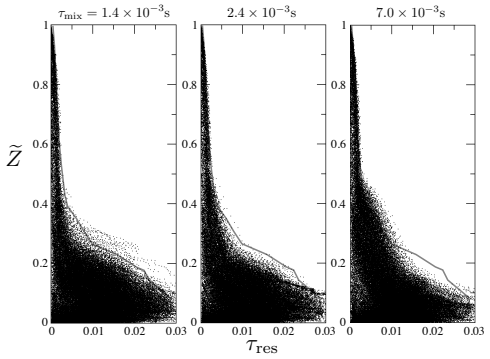

Figure 3: Scatter plots of the density-weighted average mixture fraction in the FCCT reactor against the density-weighted age (residence time), compared with the LES hull obtained in Fig. 2 (grey line).

3.2 Tabulation method

For a given τ_{mix} value, a FCCT reactor is set up as defined above, and allowed to evolve freely. Average values $\widetilde{Z}$, $\widetilde{Y_c}$ are not imposed any constraint other than the effects of the three processes. The system output, density-weighted averages of reaction and energy source terms, temperature and mass fractions, is built along the computation as a function of $\widetilde{Z}$, $\widetilde{Y_c}$ and $\tau_{\mathrm{res}} = \widetilde{a}$, by an approach of accumulation over time. Formally, if

the system composition temporal development is denoted by $\underline{\widetilde{\phi}}(t) = (\widetilde{Z}, \widetilde{Y}_c, \widetilde{a})$, the output quantities computed on a time interval $[t_0; t_f]$ are defined as

$$\widetilde{Q}(\underline{\widetilde{\phi}}^{\star}) = \frac{\int_{t_0}^{t_f} G_{\underline{\phi}}\left(\underline{\widetilde{\phi}}(t) - \underline{\widetilde{\phi}}^{\star}\right) \overline{\rho Q}(t)\, \mathrm{d}t}{\int_{t_0}^{t_f} G_{\underline{\phi}}\left(\underline{\widetilde{\phi}}(t) - \underline{\widetilde{\phi}}^{\star}\right) \overline{\rho}(t) \mathrm{d}t}\,. \tag{12}$$

In the above expression, $G_{\underline{\phi}}$ is a filter function (typically Gaussian-shaped) in the $\underline{\phi}$ space. It localizes the time integral around the target $\underline{\widetilde{\phi}}^{\star}$, meaning that only the system states at times when the Favre averages $(\widetilde{Z}, \widetilde{Y}_c, \widetilde{a})$ are close to it contribute to the output average. This definition is based on an ergodic hypothesis, according to which the average of the system evolution over time can be considered the same as an ensemble average. Behind these Favre-averaged quantities $\widetilde{Q}$ lies a distribution which is considered as the result of a turbulence-reaction history characterized by an average mixing time τ_{mix} and a residence time $\tau_{\mathrm{res}} = \widetilde{a}$. Eq. 12 is assumed to correctly define the average result of all $(\tau_{\mathrm{res}}, \tau_{\mathrm{mix}})$-controlled histories leading to the target point $(\widetilde{Z}, \widetilde{Y}_c)$. The filter size of G is set for smoothing out the noise in the raw results of the method, which are intrinsic to all Monte-Carlo-computed averages.

In practice, Eq. 12 is solved in a discrete manner, in two steps. During the run the raw data are collected on subsets of the $\underline{\phi}$ space, partitioned into $M_Z \times M_{Y_c} \times M_a$ cells, denoted by the indices (p, q, r), as illustrated in Fig. 4. Then, once the computation is finished,

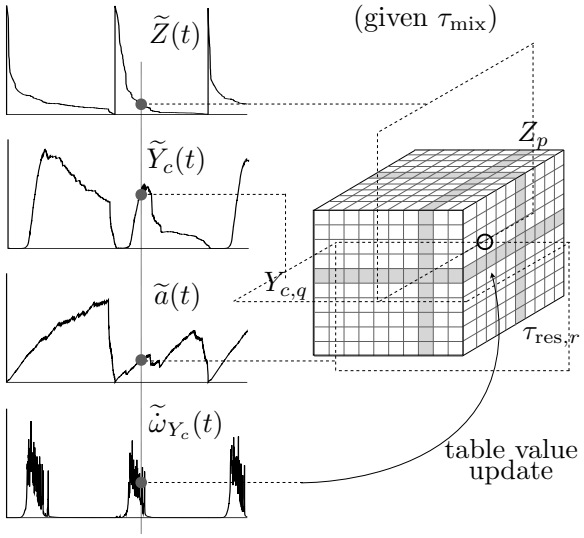

Figure 4: Schematic diagram illustrating the table construction procedure.

the Gaussian filter is applied on these $\widetilde{Q}_{p,q}$ values. The final output is a set of these Favre-averaged quantities on points $(\widetilde{Z}, \widetilde{Y}_c, \tau_{\mathrm{res}})$ of a grid covering their variation space,

indexed additionally by the mixing time value τ_{mix}, to finally make up a four-dimensional table of filtered values.

4 TABLE PROPERTIES

4.1 Distribution

A joint (Z, Y_c)-distribution obtained from an FCCT computation is plotted in Fig. 5. It corresponds to the parameter point $\widetilde{Z} = 0.177$, $\widetilde{Y}_c = 0.5 Y_{c,\text{eq}}(\widetilde{Z})$, $\tau_{\text{res}} = 3.0 \times 10^{-3}$ s and $\tau_{\text{mix}} = 2.5 \times 10^{-3}$ s. The overall segregation levels for Z and $c = Y_c / Y_{c,\text{eq}}(Z)$ are output values of the model, and equal respectively 0.28 and 0.72. A marked difference with what a presumed beta-pdf for these averages and segregations would look like is the clear dependence of the Y_c sub-distribution conditional to Z: the particles of mixture fraction smaller than 0.3 are all close to their equilibrium, whereas the richer ones are unburnt. In the PCM formulation, the Z and Y_c distributions are assumed to be independent and the SGS correlation between parameters cannot be reproduced.

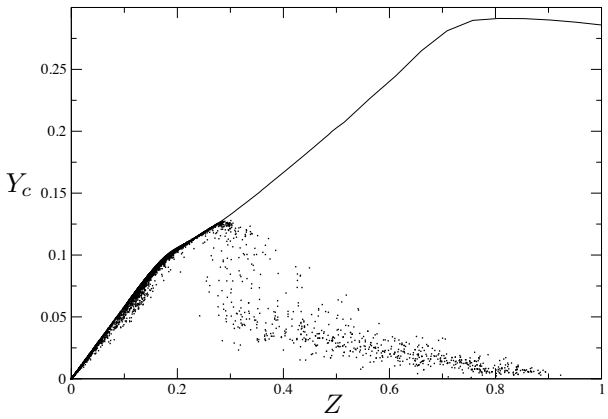

Figure 5: Fine-grained visualization of a joint (Z, Y_c)-distribution as obtained from an FCCT computation, for $\tau_{\text{res}} = 3.0 \times 10^{-3}$ s and $\tau_{\text{mix}} = 2.5 \times 10^{-3}$. Solid line: equilibrium progress variable.

4.2 FCCT output

The dependence of the output table with timescales τ_{res} and τ_{mix} is examined here. As seen in Fig. 4, during a cycle of the PaSR computation, the average mixture fraction evolves from 1 to 0. The mean injection rate is a function of this $\widetilde{Z}$ and goes decreasingly as $\widetilde{Z}$ decreases. Over one cycle, the progress variable, initially zero, increases as the reaction is enabled by the reactants' mixing, then drops again to zero, bounded by the equilibrium value $Y_{c,\text{eq}}(\widetilde{Z})$ along with $\widetilde{Z}$. The average age, τ_{res}, starts at zero and increases on average, with strong fluctuations which depend on the instantaneous injection rate. On the top of these dynamics, the mixing time τ_{mix} enhances the homogenization of the mixture: the Z variance is a more strongly decreasing function of τ_{res} for smaller τ_{mix}

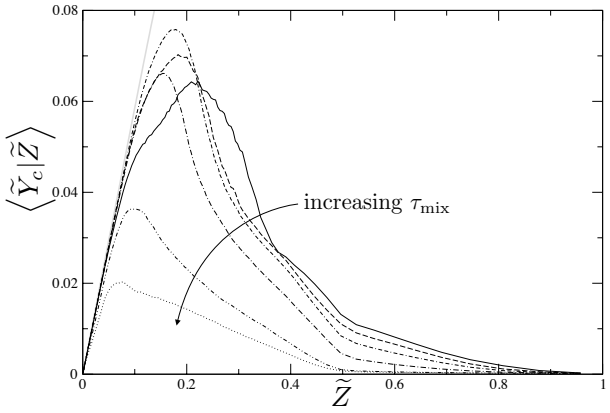

Figure 6: Time average of the density-weighted mean progress variable in the FCCT reactor, conditioned by the average mixture fraction. The increasing mixing timescale values vary from 8×10^{-4} to 1.6×10^{-2}s. Grey line: equilibrium.

values. If the mixing is infinitely fast, that is if $\tau_{\text{mix}} \ll \tau_{\mathcal{R}}$ and $\tau_{\text{mix}} \ll \tau_{\text{che}}$, the reactor behaves as a homogeneous point, the Z variance is zero and a laminar behavior is retrieved. This corresponds to the DNS limit in the simulations: Δ^2 small or D_t large. The output averages then reproduce merely the interaction between chemistry and the local laminar diffusion-transport phenomena, rendered in the reactor by the $\tau_{\mathcal{R}}$ law. At higher τ_{mix} values, the mixing starts to interact with the injection process and, because of the mixture fraction distribution spread around its average, reaction may be enhanced or slowed down, depending on the chemical properties. In Fig. 6, the time average of the mean-progress variable is plotted as a function of $\widetilde{Z}$ for an increasing sequence of τ_{mix} values. It appears that around stoichiometry, increasing the mixing time leads to a mixture burning first more easily, up to a maximum, and then quenching (for a given $\widetilde{Z}$, $\left\langle \widetilde{Y}_c|\widetilde{Z} \right\rangle$ increases then decreases). When τ_{mix} becomes very large compared to the injection timescale, fuel and oxydizer remain fully segregated over a cycle and no burning is possible.

As far as the chemical source terms are concerned, the reaction-enhancing role of the mixing is evidenced in Fig. 7, where the average progress variable source term at stoichiometry is plotted against τ_{mix} and τ_{res}. It appears that the smaller τ_{mix}, the quicker the reaction occurs, with higher $\widetilde{\dot{\omega}}_{Y_c}$ values, shorter ignition times (τ_{res} at which the maximum source term is reached) and longer reaction durations.

5 RESULTS IN AN LES

An FCCT table is computed for the inlet conditions of the lifted methane-air jet flame experiment by Cabra et al. (2005). It is carried out using 100×100 points in the Z and Y_c directions, and 16 points for each of the residence and mixing time parameters, over 3×10^7 time steps for each τ_{mix} value, which takes about 11 hours on 64 cores of an IBM Power6 server.

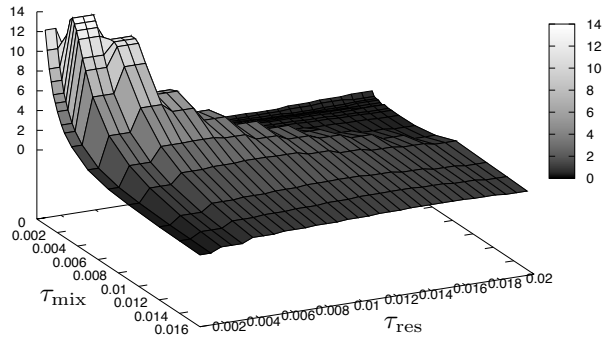

Figure 7: Filtered chemical source term $\widetilde{\dot{\omega}}_{Y_c}$ at stoichiometry in the variable-age FCCT reactor configuration, averaged in time and over the whole progress variable range, plotted as a function of τ_{mix} and τ_{res}.

Instantaneous fields of the resulting temperature and energy source term, as well as the mixture fraction segregation – an output of the model–, are presented in Fig. 8. The flame positions itself steady around 40–50 jet diameters, in conformity with the experimental observation. The progress variable and energy source terms are of equivalent order of magnitude as those found in computations using PCM, like those by Domingo et al. (2008).

6 CONCLUSIONS

The method presented in this work introduces the use of a residence time and a mixing time in the SGS modeling of turbulent combustion for LES. Subgrid-scale distributions are built by discrete PaSR simulations of the characteristic flow evolutions of the interaction between mixing and chemistry, and are directly used in the simulation as a look-up table of filtered chemical quantities. This approach prevents the need for inaccurate statistical assumptions laid directly on the distributions (as necessary in presumed pdf methods), thus offering the prospect of addressing multi-parameter problems, e.g. multiple inlet, variable enthalpy, or local dilution by burnt gases.

The challenge lays in the modeling, in the composition space, of the flow dynamics; to that purpose, the residence and mixing times, part of an easily computable class of scalars, prove to be relevant conditioning variables for the case presented in this study of a lifted jet flame LES simulation. Further developments will include a refinement and systematization of the characterization of the PaSR model properties which accurately reproduce the chemistry-turbulence interaction observed in the flow.

ACKNOWLEDGEMENTS

Financial support by the ADEME and the Air Liquide Group through Project SAFIR (Simulation Avancée de Foyers Industriels avec Recycle) is gratefully acknowledged. This

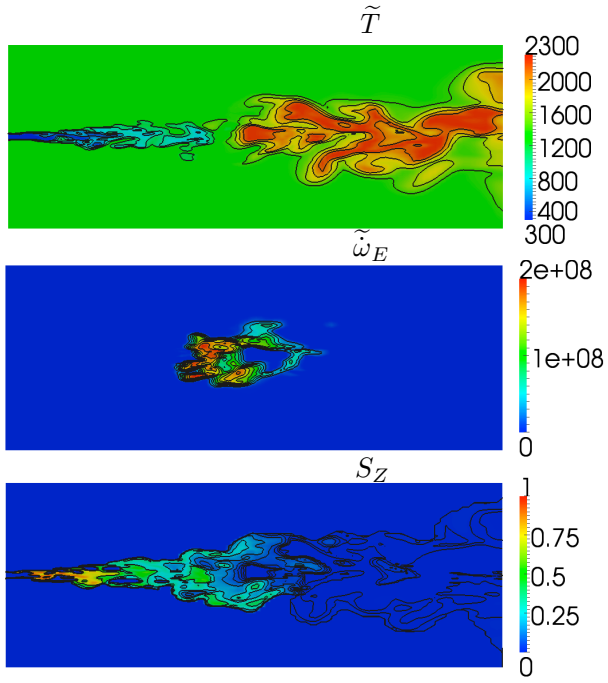

Figure 8: From top to bottom, instantaneous fields of temperature (K), energy source term (W.m^{-3}) and subgrid Z segregation (linear color scale, logarithmic isolines) as obtained from the LES using the FCCT table.

work was granted access to the HPC resources of IDRIS under the allocation 2009-020152 made by GENCI.

REFERENCES

[1] F.A. Jaberi, P.J. Colucci, S. James, P. Givi and S.B. Pope, Filtered mass density function for large-eddy simulation of turbulent reacting flows, *J. Fluid Mech.*, **401**, 85–121 (1999).

[2] L. Vervisch, R. Hauguel, P. Domingo and M. Rullaud, Three facets of turbulent combustion modelling: DNS of premixed V-flame, LES of lifted nonpremixed flame and RANS of jet-flame, *J. Turbulence*, **5** (4), 1–36 (2004).

[3] O. Gicquel, D. Thevenin, M. Hilka M. and N. Darabiha, Direct numerical simulation of turbulent premixed flames using intrinsic low-dimensional manifolds, *Combust. Th. Modelling*, V**3**, 479–502 (1999).

[4] F. Ghirelli, B. Leckner, Transport equation for the local residence time of a fluid, *Chem. Eng. Sci.*, **59**, 513–523 (2004).

[5] A.Y. Klimenko, On simulating scalar transport by mixing between Lagrangian particles, *Phys. Fluids*, **19**, 031702.

[6] P. Domingo, L. Vervisch, S. Payet and R. Hauguel, DNS of a premixed turbulent V flame and LES of a ducted flame using a FSD-PDF subgrid scale closure with FPI-tabulated chemistry, *Combust. Flame*, **143**, 566–586 (2005).

[7] P. Domingo, L. Vervisch and D. Veynante, Large-eddy simulation of a lifted methane jet flame in a vitiated coflow, *Combust. Flame*, **152**, 415–432 (2008).

[8] G. Godel, P. Domingo and L. Vervisch, Tabulation of NO_x chemistry for Large-Eddy Simulation of non-premixed turbulent flames, *Proc. Combust. Inst.*, **32**, 1555–1561 (2009).

[9] R. Cabra, J. Chen, R. Dibble, A. Karpetis and R. Barlow, Lifted methane-air jet flames in a vitiated coflow, *Combust. Flame*, **117**, 732–754 (2005).

[10] Z. Ren and S.B. Pope, An investigation of the performance of turbulent mixing models, *Combust. Flame*, **136**, 208–216 (2004).

[11] Z. Ren and S.B. Pope, Second-order splitting schemes for a class of reactive systems, *J. Comput. Phys.*, **227**, 8165–8176 (2008).

[12] S. Subramaniam and S.B. Pope, A mixing model for turbulent reacting flows based on Euclidian Minimum Spanning Trees, *Combust. Flame*, **115**, 487–514 (1998).